Theoretical Studies on Cycloaddition Reactions of 2-Azaallene Cations with Isocyanates

Si-Ya Yang,[a,b] Cheng-Ke Sun,[a,b] and De-Cai Fang*[a]

Keywords: Density functional theory / 2-Azaallene cations / Isocyanates / Reaction mechanisms

The mechanisms of cycloaddition reactions between 2-azaallene cations and isocyanates have been explored at the B3LYP/6-31G* level. It is found that [2+2] or [2+4] cycloaddition reactions can take place via an intermediate when 2-azaallene cations react with 1 or 2 equiv. of isocyanates. The effects of substituents are also reported in the present paper, and the results obtained indicate that electron-attracting groups on 2-azaallene cations favor the reaction, and electron-donating groups on 2-azaallene cations hinder the reaction. Substituents on isocyanates have the opposite effects. These results have been rationalized with FMO interaction.

Introduction

Cycloaddition reactions between cumulenes and double-bond compounds are very important routes for the synthesis of cycloadducts. In the past decades, [2+2] cycloaddition reactions of ketenes, ketenimines, allenes, and keteniminium cations have been extensively studied theoretically[1−4] and experimentally.[5−6] Our previous papers[4,7] indicate that the mechanisms of cycloaddition reactions involving keteniminium or 2-azaallene cations are quite complicated, and many intermediate species have been located. 2-Azaallene cations, as a class of heterocumulenes, are very reactive, giving rise to heterocycles and open-chain compounds.[8−11] In 1995, Ismail et al. reported the experimental results of [2+2] and [2+4] cycloaddition reactions of 2-azaallene salts with isocyanates, which provide a new route for the preparation of heterocycles and less-conventional open-chain compounds.[12]

To the best of our knowledge, there has been no theoretical study of the reaction mentioned in the title of this article. Therefore, we present DFT studies on the mechanisms for reactions of the 2-azaallene cation with one isocyanate molecule or two isocyanate molecules. We have also investigated substituent effects on these reactions. The reactions considered are shown in Scheme 1.

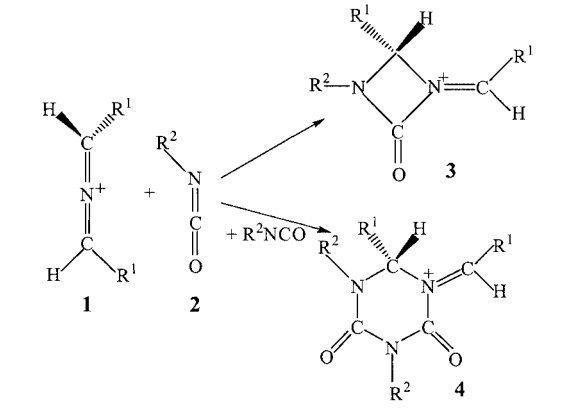

	1a	1b	1c	2a	2b	2c	3a	3b	3c	3d	3e	4a	4b	4c	4d	4e
R^1	H	Cl	CH_3				H	Cl	CH_3	H	H	H	Cl	CH_3	H	H
R^2				H	Cl	CH_3	H	H	H	Cl	CH_3	H	H	H	Cl	CH_3

Scheme 1

The Z-matrixes, energetics (total energies and ZPEs) of all the stationary points are listed in Tables S1−S8 of the Supporting Information, along with the numbering systems in Figures S1−S4 (see footnote on page 1 of this article).

Results and Discussion

The Prototype Reaction: $H_2C{=}N^+{=}CH_2$ + HN=C=O and $H_2C{=}N^+{=}CH_2$ + 2 HN=C=O

First we considered the reaction $H_2C{=}N^+{=}CH_2$ + HN=C=O, in which the geometries of reactants (**1a** and

[a] Department of Chemistry, Beijing Normal University, Beijing 100875, China
Fax: (internat.) + 86-10/62200567
E-mail: dcfang@bnu.edu.cn
[b] Department of Chemistry, Qujing Normal College, Qujing 655000, China

Supporting information for this article is available on the WWW under http://www.eurjoc.org or from the author.

  DOI: 10.1002/ejoc.200200650

2a), complex (**COM1a**), intermediate (**INT1a**), transition states (**TS1a**, **TS2a**), and product (**3a**) are optimized at the B3LYP/6-31G* and MP2/6-31G* levels. The numbering systems of the stationary points are shown in Scheme 2 and the geometries obtained are listed in Table S1 of the Supporting Information, which indicate that both calculation methods (B3LYP and MP2) give similar results.

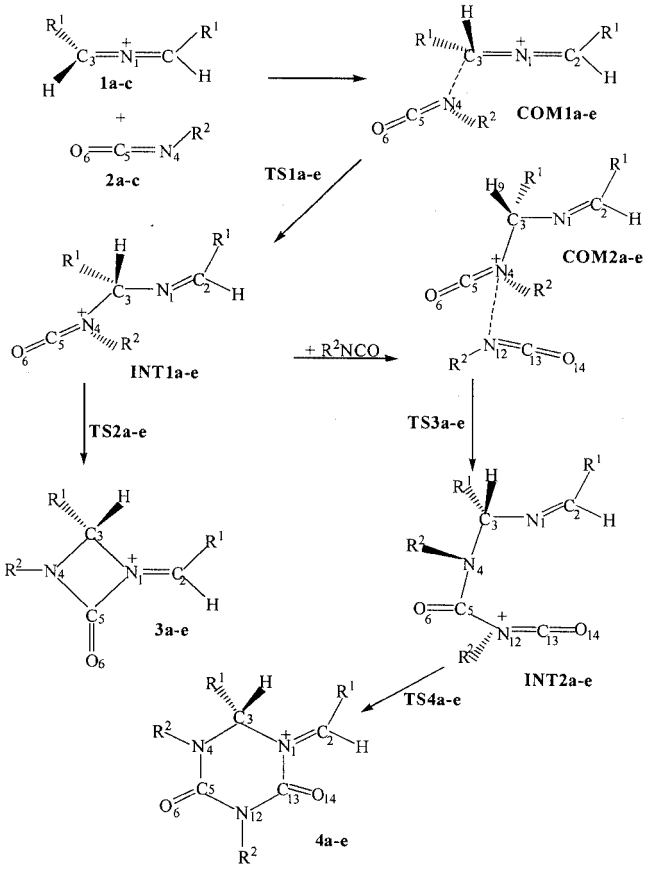

Scheme 2

The structural parameters reveal that one reactant, the 2-azaallene cation (**1a**), is a linear molecular with its skeleton atoms in the same plane, while the two methylene planes are perpendicular to each other. The obtained bond length and angle are in reasonable agreement with those reported by Böttger et al.[18] in 1997 at the B3LYP/6-31+G* level. The skeleton atoms in the four-membered ring product **3a** are in the same plane, but the two hydrogen atoms attached to C^3 are distributed above and below the plane (see Figure S1 and Table S1 of the Supporting Information).

When reactant **2a** approaches **1a**, complex **COM1a** is formed owing to the favorable electrostatic interaction of the reactants (the charges of N^4 and C^3 are −0.26 and +0.53 e, respectively), with the bond length of N^4-C^3 being 2.68 Å at the B3LYP/6-31G* level. After **COM1a**, intermediate **INT1a** is formed via a transition state, **TS1a**. The C^3-N^4 and C^5-N^1 distances in **TS1a** are 1.84 and 3.70 Å, respectively, and the angle $C^2-N^1-C^3$ in **TS1a** becomes 142.6° from the original 180.0° in **1a**. As the reactants approach further, **TS1a** becomes intermediate **INT1a**, in which the bond lengths of C^3-N^4 and C^4-N^1 are 1.54 and 3.52 Å, respectively. In **TS2a**, the dihedral angle $C^5-N^4-C^3-N^1$ becomes 110.3°, 47° less than that in **INT1a**, and the C^5-N^1 distance is slightly shorter (3.31 Å). After **TS2a**, the reaction yields a four-membered ring product **3a**, in which the bond lengths of C^3-N^4 and C^5-N^1 are 1.46 and 1.59 Å, respectively.

The relative energies of the stationary points are given in Figure 1 (with zero-point energy correction), which shows that as **COM1a** is formed, the reaction first releases 8.1 kcal/mol energy (only 7.3 kcal/mol with BSSE correction) and then overcomes an energy barrier of 11.9 kcal/mol (12.9 kcal/mol with BSSE correction) to form **INT1a**, which is the rate-controlling process. Figure 1 also shows that **INT1a** is an unstable intermediate and easily changes to the adduct **3a**, whose energy barrier is only about 0.9 kcal/mol (with ZPE) at the B3LYP/6-31G* level.

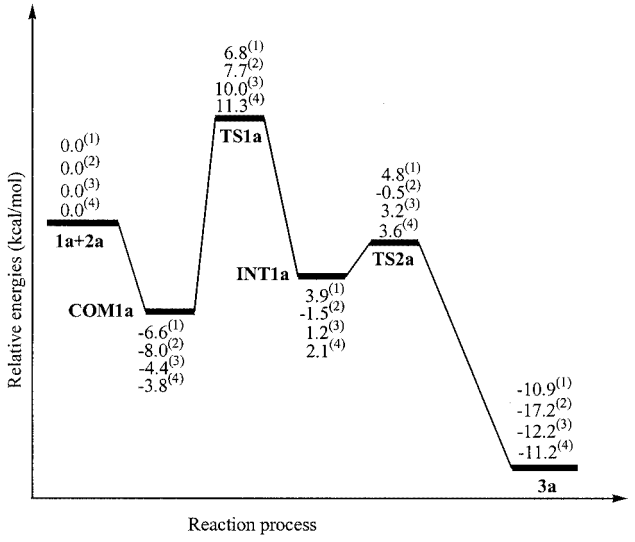

Figure 1. Schematic description of the potential energy surface for the reaction of **1a** + **2a** [(1) B3LYP/6-31G*+ZPE(B3LYP), (2) MP2/6-31G*+ZPE(MP2), (3) CCSD(T)/6-31G*//B3LYP+ZPE(B3LYP), (4) CCSD(T)/6-31+G*//B3LYP+ZPE(B3LYP)]

After **INT1a**, there are two possiblities. One is to form adduct **3a** as discussed above; the other is that **INT1a** can further react with excess HN=C=O to form the six-membered ring product **4a**. For the latter process we have located a complex (**COM2a**), one intermediate (**INT2a**), two transition states (**TS3a**, **TS4a**) and one product (**4a**) at both B3LYP/6-31G* and MP2/6-31G* levels (see Figure S1 and Table S1 of the Supporting Information).

An intermolecular complex **COM2a** forms first when **INT1a** reacts with an HN=C=O molecule. In **COM2a**, the lengths of C^5-N^{12} and $N^{12}-H^9$ are 2.80 and 2.45 Å and the $C^5-N^4-C^3-N^1$ and $C^{13}N^{12}C^5N^4$ are 166.74 and −109.34°, respectively. As the reaction proceeds, the hydrogen bond in **COM2a** is destroyed first and then intermediate **INT2a** is formed via a transition state **TS3a**. The geometry of **TS3a** is somewhat similar to **COM2a**, but the C^5-N^{12} distance is only 1.94 Å, 0.86 Å shorter than in

COM2a and 0.3 Å longer than that in **INT2a**. As the dihedral angle of $C^5-N^4-C^3-N^1$ changes, the ring closure of **INT2a** produces a six-membered ring adduct **4a** via **TS4a**.

Because C^5 in **INT1a** carries a higher charge (+0.82 e) and the N^{12} atom in the HN=C=O molecule has a negative charge (−0.26 e), **COM2a** has 5.9 kcal/mol less energy than **INT1a**+**2a** at the B3LYP/6-31G*+ZPE level as shown in Figure 2, which shows that the energy barrier for the step from **COM2a** to **INT2a** is 2.1 kcal/mol while that for the step from **INT2a** to **4a** is 1.0 kcal/mol at the B3LYP/6-31G* level, i.e., the [2+4] cycloaddition reaction can take place quite easily. If BSSE is considered, the energy barrier for the process from **COM2a** to **INT2a** will become 2.7 kcal/mol, 1.8 kcal/mol higher than for the process from **INT1a** to **3a**.

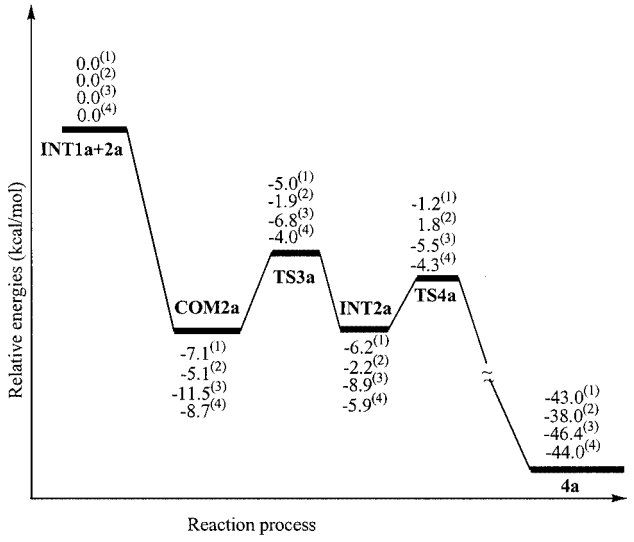

Figure 2. Schematic description of the potential energy surface for the process from **INT1a** + **2a** to **4a** [(1) B3LYP/6-31G*+ZPE(B3LYP), (2) MP2/6-31G*+ZPE(MP2), (3) CCSD(T)/6-31G*//B3LYP+ZPE(B3LYP), (4) CCSD(T)/6-31+G*//B3LYP+ZPE(B3LYP)]

In both [2+2] and [2+4] reactions, the rate-controlling steps (the formation of **INT1a**) are the same, but if one wants to discuss the ratio of products **3a** and **4a**, one might calculate the rates of reaction for processes from **INT1a** to **3a**, from **COM2a** to **INT2a** or from **INT2a** to **4a**. In fact, the [2+4] process is unfavorable for both enthalpic and entropic reasons. The change of entropy ($\Delta S^{\neq}$) for the process from **INT1a** to **3a** is $-2.4\ \mathrm{cal\cdot mol^{-1}\cdot K^{-1}}$, while those for the processes from **COM2a** to **INT2a** and from **INT2a** to **4a** are −10.9 and $-8.3\ \mathrm{cal\cdot mol^{-1}\cdot K^{-1}}$, respectively. Such differences will contribute to the change in Gibbs free energy ($\Delta G^{\neq}$) of about 2.5 (from **COM2a** to **INT2a**) or 1.7 kcal/mol (from **INT2a** to **4a**) even at room temperature (298 K), which is large enough to influence the reaction rate of the low-energy-barrier reaction. Therefore, as was pointed out by a referee, the reaction $H_2C=N^+=CH_2$ + 2 HN=C=O must be entropically hindered. From transition state theory, we calculated that the reaction rate for the process from **INT1a** to **3a** is $7.66\cdot10^{11}\ \mathrm{s^{-1}}$, while those for the processes from **COM2a** to **INT2a** and from **INT2a** to **4a** are $9.69\cdot10^{9}$ and $7.68\cdot10^{7}\ \mathrm{s^{-1}}$ respectively. So our present results are in good agreement with Ismail's experimental result that even with excess (2−5 equiv.) of isocyanate, the 2-azaallene cation will react in a 1:1 ratio to form a four-membered ring product.[12]

In order to study the basis set and correlation energy effects, single-point energy calculations of CCSD(T)/6-31G*//B3LYP/6-31G* and CCSD(T)/6-31+G*//B3LYP/6-31G* have been performed at the optimized stationary points. The relative energies of these methods are given in Figures 1 and 2, which indicate that the relative energies in the prototype reaction are similar at B3LYP, MP2, and CCSD(T) calculation levels and the biggest difference is about 4 kcal/mol, i.e., B3LYP/6-31G* is reliable for the present study. Therefore, only the B3LYP/6-31G* method has been employed in the later study of the effects of substituents.

To study the bonding character and charge distribution for the intermolecular weak interactions, electron density analysis has been carried out with B3LYP/6-31G* wavefunctions. Laplacian distributions of **TS1a**, **INT1a**, **COM2a**, and **TS3a** are illustrated in Figure 3, which indicates that there are two critical points between the reactants in **COM2a**. One is that between C^5 and N^{12}, the other between N^{12} and H^9. The electron densities ρ_b for the C^5-N^{12} and $N^{12}-H^9$ bonds are 0.013 and 0.01 in **COM2a**, which means that these bonds are quite weak. However, in **TS3a**, the bond critical point between N^{12} and H^9 disappears and the C^5-N^{12} bond becomes stronger (ρ_b = 0.04). In **TS1a**, the electron density ρ_b for the bond N^4-C^3 to be formed is 0.1, which is mainly caused by electron donation from the nitrogen atom in the HNCO molecule, the same as the FMO interaction shown in Scheme 3. However, in **INT1a** the electron density ρ_b for the bond N^4-C^3 is 0.208, and a single bond has been formed as illustrated in Figure 3.

Effects of Substituents on the Carbon Atom in the 2-Azaallene Cation

To study the influence of substituents on the carbon atoms in the 2-azaallene cation, we tried to investigate the reactions of 1,3-dichloro-2-azaallene and 1,3-dimethyl-2-azaallene with HNCO, i.e., the reaction **1b** + **2a** and **1c** + **2a**. The numbering systems are illustrated in Scheme 2, and the complete reaction scheme (see Scheme 2), as discussed in the model reaction, is also considered here.

Because larger groups such as Cl or CH_3 are attached to the terminal carbon atoms of 2-azaallene, we could not locate intermolecular complexes similar to **COM1a**, but in each case a hydrogen-bonded complex could be found, which is confirmed by topological analysis shown in Figure 3. The electron-attracting effect of the Cl group leads to a slightly more active C−H bond in 2-azaallene, and thus **COM1b** is more stable than **COM1c** (see Figure 4). Just like the model reaction, two transition states (**TS1b** and **TS2b** or **TS1c** and **TS2c**) and one intermediate (**INT1b** or **INT1c**) have been located for each substituted reaction. From Figure 4, one can see that the Cl atom, an electron-

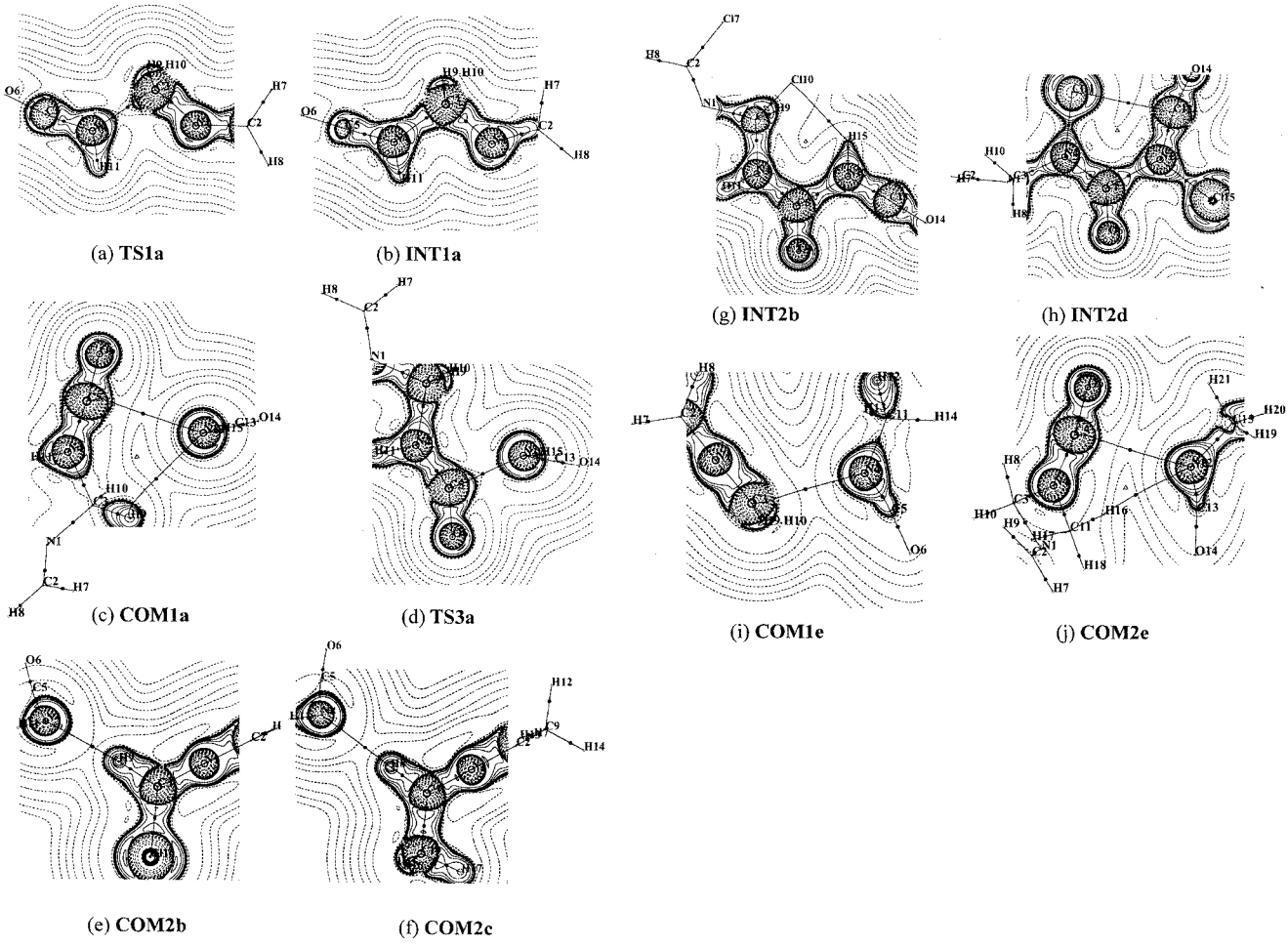

Figure 3. Molecular graphs and Laplacian distribution of the stationary points in the studied reaction; in these figures, dashed lines denote positive values of $\nabla^2\rho_b$ and full lines stand for negative values of $\nabla^2\rho_b$; bonded charge concentrations are indicated by solid squares; in addition, bond paths (heavy solid lines), bond critical points (solid circle) and ring critical points (triangle) are shown for $\rho(r)$

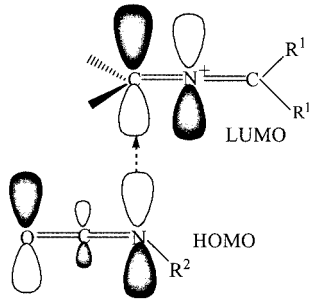

Scheme 3

attracting substituent, favors the reaction. The energy of **TS1b** is only 3.8 kcal/mol above **1b**+**2a** and 11.9 kcal/mol above **COM1b** (with ZPE correction). On the contrary, the CH_3 group, an electron-donating substituent, reduces the ease with which the reaction proceeds. The energy of **TS1c** is 18.4 and 22.7 kcal/mol above the reactants and **COM1c**, respectively, much higher than in the model reaction. Thus, we can conclude that electron-attracting substituents on a 2-azaallene cation favor the reaction while electron-donating substituents on a 2-azaallene cation inhibit the reaction. This conclusion can be inferred from the frontier orbital interaction (FMO) as shown in Scheme 3, because the electron-attracting groups lower the energy level of the LUMO of the 2-azaallene cation, and lower the energy gap between the HOMO of HNCO and the LUMO of the 2-azaallene cation. Obviously, electron-donating groups have the opposite effects. So we can conclude that 1,3-dichloro-2-azaallene is more reactive than 1,3-dimethyl-2-azaallene, which might be one reason why Ismail et al. selected 1,3-dichloro-2-azaallene salts as one of the reactants in their experiments.[12]

When HNCO is in excess, the intermediates **INT1b** or **INT1c** could combine with another HNCO to form a molecular complex **COM2b** or **COM2c**. In these complexes, there are two weak intermolecular interactions, N···C and N···H−C (the same as Figure 3, c), but the $N^{12}-C^5$ distance in **COM2b** is 0.18 Å shorter than that in **COM2c** (2.95 Å). The mechanisms of these reactions are the same as those of the model reaction.

Owing to the disappearance of N···H−C bonds in **TS3c**, the energy barrier (4.0 kcal/mol) from **COM2c** to **INT2c** is higher than that from **COM2b** to **INT2b** (0.1 kcal/mol) as shown in Figure 5. In **TS3b**, the hydrogen bond N···H−C

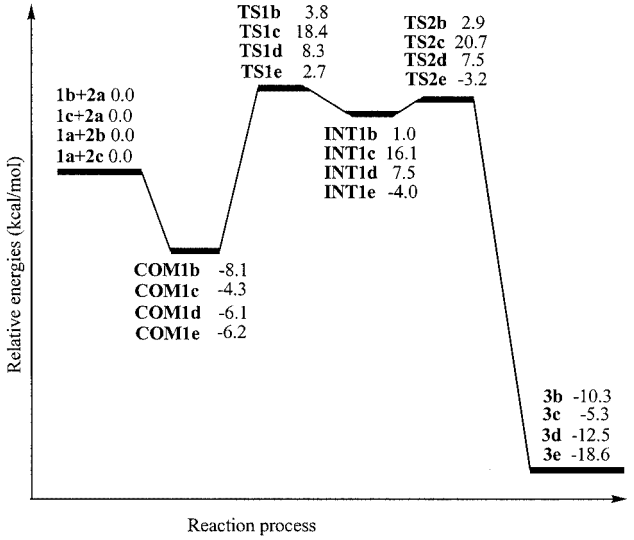

Figure 4. The schematic description of potential energy surfaces for **1b** + **2a**, **1c** + **2a**, **1a** + **2b**, and **1a** + **2c** reactions at the B3LYP/6-31G* level (with ZPE correction)

is still present. With the further approach of reactants to each other, the $N^{12}\cdots H^{9}-C$ bond is broken, but another intermolecular hydrogen bond (ρ_b = 0.027) between Cl^{10} and H^{15} forms in **INT2b** (see Figure 3), which makes **INT2b** more stable than other corresponding intermediates. For example, the relative energy of **INT2b** is 12.1 kcal/mol lower than that of **INT2c** (see Figure 5).

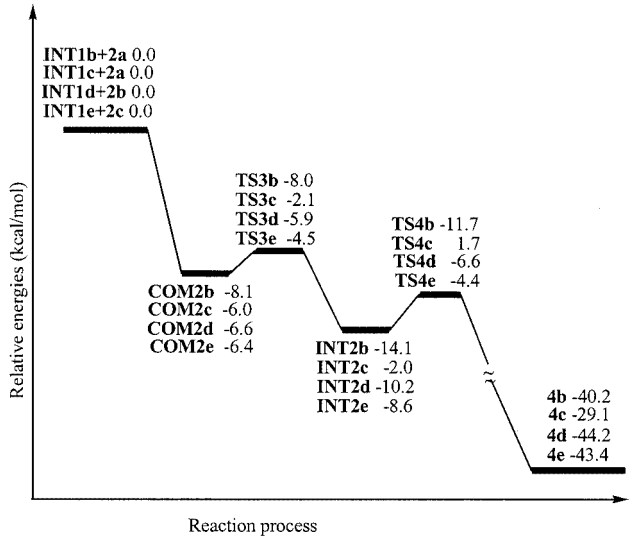

Figure 5. The schematic description of potential energy surfaces for [2+4] reaction processes at the B3LYP/6-31G*+ZPE level

Effects of Substituents on the Nitrogen Atom in Isocyanates

In this section, we report our studies of the effects of substituents on the nitrogen atom in isocyanates (see Scheme 2). We chose two types of substituents (Cl and CH_3) and we also considered both four- and six-membered ring products.

For the reaction of **1a** + **2b** or **1a** + **2c** (see Scheme 2), we have located all the possible transition states and intermediates, which are denoted as **COM1d**, **TS1d**, **TS2d**, **INT1d** and **COM1e**, **TS1e**, **TS2e**, **INT1e**, respectively. These stationary points are also further confirmed by vibrational analysis, and the transition states are characterized by the only imaginary frequency. The numbering systems are given in Scheme 2.

For reaction **1a** + **2b**, the optimized parameters for **COM1d**, **TS1d**, **INT1d**, and **TS2d** are similar to those of the corresponding stationary points in the model reaction. As far as the energy is concerned, the energy of **TS1d** is 8.3 and 14.4 kcal/mol above **1a**+**2b** and **COM1d**, respectively, which are slightly higher than those in model reaction **1a**+**2a** (see Figures 1 and 4). This situation can be explained by frontier orbital interaction (see Scheme 3). When an electron-attracting substituent (such as Cl) is attached to the N atom in an isocyanate, the energy level of the HOMO in the isocyanate will be slightly lower than that in HN=C=O, which will increase the energy gap between the HOMO of the isocyanate and the LUMO of the azaallene cation.

However, for the reaction **1a** + **2c**, a molecular complex **COM1e** is formed first, which has about 6.2 kcal/mol stabilization energy. Figure 4 indicates that **TS1e** is only 2.7 kcal/mol above the reactant asymptote and the energies of all other stationary points along this reaction path are well below the reactant **1a**+**2c**. Because an electron-donating CH_3 group in the isocyanate will promote the energy level of the isocyanate HOMO, it will decrease the energy gap between the HOMO of isocyanate and the LUMO of the 2-azaallene cation and thus favor the interaction shown in Scheme 3. In Ismail's experiments,[12] only electron-donating groups were chosen for study, which is in good agreement with our present results.

When **2b** and **2c** are in excess, the intermediates **INT1d** and **INT1e** can further react to form the last six-membered products **4b** and **4c**. The corresponding molecular complexes **COM2d** and **COM2e** are also located at the beginning of the reaction **INT1d** + **2b** and **INT1e** + **2c**. There is nothing special about **COM2d**, but the structures of **INT2d** and **COM2e** are somewhat different. Topological analysis indicates that a weaker interaction exists between Cl^{11} and C^{13} in **INT2d**, which might explain why **INT2d** is about 14.1 kcal/mol lower in energy than **INT1d**+**2b**. In **COM2e**, interactions occur between $C^{5}\cdots N^{12}$ and $N^{12}\cdots H^{16}$, as shown in Figure 3. The relative energies show that [2+4] reaction processes are quite easy because complexation of the intermediate with HNCO is exothermic to the extent of 6−8 kcal/mol, which is sufficient for overcoming the later activation barriers.

Conclusions

For the model reaction, the reaction proceeds to form an initial intermediate, and the intermediate can then either undergo cyclization to form a four-membered ring adduct or combine with another HNCO to form a six-membered ring product.

Electron-attracting substituents on the carbon atom of a 2-azaallene cation (as in the 1,3-dichloro-2-azaallene cation) have a positive influence on the rates of reactions, but electron-donating substituents on the 2-azaallene cation (as in 1,3-dimethyl-2-azaallene) inhibit the reaction.

When substituents are on the nitrogen atom of an isocyanate, they have the opposite effects. Electron-donating groups favor the reaction, which is in good agreement with the FMO interaction.

The calculated activation barriers of the title reactions are quite low, which is in agreement with the experimental fact that these reactions between the 2-azaallene cation (or its salts) and isocyanates can occur at room temperature.

Experimental Section

Computational Method and Models: All the calculations included in this work have been performed with the Gaussian 98w program.[13] For the model reaction, the geometries of reactants, products, complexes, intermediates, and transition states of the title reaction have been fully optimized at B3LYP/6-31G* and MP2/6-31G* levels, and single-point energies of the title reaction have been recomputed at CCSD(T)/6-31G*//B3LYP/6-31G* and CCSD(T)/6-31+G*//B3LYP/6-31G* levels. All stationary points have been further confirmed by the computation of force constants analytically and characterized by the number of imaginary vibrational frequencies. IRC has also been traced with B3LYP/6-31G* for the model reaction, which shows that the transition states are on the right potential energy surface. For the substituted reactions, only B3LYP/6-31G* has been used to locate the geometric parameters in order to save CPU time. Bader's theory of AIM[14,15] has been used to study the bonding character and charge distribution for the complexes, some transition states and intermediates. The AIM98PC package,[16] a PC version of AIMPAC,[17] has been employed for the electron density topological analysis using the electron densities obtained with B3LYP/6-31G* calculations.

Acknowledgments

This project was supported by National Natural Science Foundation of China (No. 20073006). S.-Y. Y. and C.-K. S. also thank the Natural Science Foundation of Qujing Normal College (No. 0113908).

[1] For example: [1a] J. A. Sordo, J. González, T. L. Sordo, *J. Am. Chem. Soc.* **1992**, *114*, 6249−6251. [1b] X. Assfeld, J. A. Sordo, J. González, M. F. Ruiz-López, T. L. Sordo, *J. Mol. Struc. (Theochem)*. **1993**, *287*, 193−199. [1c] R. López, T. L. Sordo, J. A. Sordo, J. González, *J. Org. Chem.* **1993**, *58*, 7036−7037. [1d] R. López, D. Suárez, M. F. Ruiz-López, J. A. Sordo, T. L. Sordo, *J. Chem. Soc., Chem. Commun.* **1995**, 1677−1678. [1e] R. López, M. F. Ruiz-López, D. Rindaldi, J. A. Sordo, T. L. Sordo, *J. Phys. Chem.* **1996**, *100*, 10600−10608.

[2] For example: [2a] F. P. Cossio, J. M. Ugalde, X. López, B. Lecea, C. Palomo, *J. Am. Chem. Soc.* **1993**, *115*, 995−1004. [2b] F. P. Cossio, A. Arrieta, B. Lecea, J. M. Ugalde, *J. Am. Chem. Soc.* **1994**, *116*, 2085−2093. [2c] B. Lecea, I. Arrasta, A. Arrieta, G. Roa, X. López, M. I. Arriortua, J. M. Ugalde, F. P. Cossio, *J. Org. Chem.* **1996**, *61*, 3070−3079. [2d] D. C. Fang, X. Y. Fu, *Int. J. Quantum Chem.* **1994**, *50*, 93−99. [2e] D. C. Fang, X. Y. Fu, *Int. J. Quantum Chem.* **1996**, *57*, 1107−1114.

[3] For example: [3a] W. M. F. Fabian, R. Janoschek, *J. Am. Chem. Soc.* **1997**, *119*, 4253−4257. [3b] D. C. Fang, X. Y. Fu, *Chem. Phys. Lett.* **1996**, *259*, 265−270. [3c] W. M. F. Fabian, G. Kollenz, *J. Org. Chem.* **1997**, *62*, 8497−8502. [3d] M. Alajarin, A. Vidal, F. Tovar, A. Arrieta, B. Lecea, F. P. Cossio, *Chem. Eur. J.* **1999**, *5*, 1106−1117. [3e] P. Wu, S. R. He, *J. Beijing Norm. Univ. (Nature Sci.)* **1999**, *35*, 90−92. [3f] D.-C. Fang, H.-M. Li, *J. Mol. Struc.* **2000**, *528*, 111−119. [3g] W. M. F. Fabian, G. Kollenz, *J. Phys. Org. Chem.* **1994**, *7*, 1−9. [3h] A. Arrieta, F. P. Cossio, *J. Org. Chem.* **1999**, *64*, 1831−1842.

[4] W. J. Ding, D. C. Fang, *J. Org. Chem.* **2001**, *66*, 6673−6678.

[5] For example: [5a] D. Bellus, B. Ernst, *Angew. Chem.* **1988**, *100*, 820−850; *Angew. Chem. Int. Ed. Engl.* **1988**, *27*, 797−827. [5b] B. B. Snider, *Chem. Rev.* **1988**, *88*, 793−811. [5c] G. I. Georg, V. T. Ravikumar, in: *The Organic Chemistry of β-Lactams* (Ed.: G. I. Georg), VCH, New York, **1993**.

[6] For some keteniminium cation systems: [6a] L. Ghosez, *Angew. Chem. Int. Ed. Engl.* **1972**, *11*, 852−853. [6b] J. B. Falmagne, J. Escudero, S. Taleb-Sahraoui, L. Ghosez, *Angew. Chem. Int. Ed. Engl.* **1981**, *20*, 879−880. [6c] C. Genicot, B. Gobeaux, L. Ghosez, *Tetrahedron Lett.* **1991**, *32*, 3827−3830. [6d] O. Irie, K. Shishido, *Chem. Lett.* **1995**, 53−54. [6e] G. Barbaro, A. Battaglia, C. Btuno, P. Giorgianni, A. Guerrini, *J. Org. Chem.* **1996**, *61*, 8480−8488. [6f] P. J. Shim, H. D. Kim, *Tetrahedron Lett.* **1998**, *39*, 9517−9520. [6g] J.-M. Adam, L. Ghosez, K. N. Houk, *Angew. Chem. Int. Ed.* **1999**, *38*, 2728−2730.

[7] S. Y. Yang, C. K. Sun, D. C. Fang, *J. Org. Chem.* **2002**, *67*, 3841−3846.

[8] E.-U. Würthwein, *J. Org. Chem.* **1984**, *49*, 2971−2978.

[9] J. C. Jochims, A. Hamed, T. Huu-phuoc, J. Hofmann, H. Fischer, *Synthesis* **1989**, 918−920.

[10] A.-H. Ismail, A. Hamed, I. Zeid, J. C. Jochims, *Tetrahedron* **1992**, *48*, 8271−8274.

[11] A. Hamed, *Synthesis* **1992**, 591−595.

[12] A.-H. Ismail, A. Hamed, M. G. Hitzler, C. Troll, J. C. Jochims, *Synthesis* **1995**, 820−826.

[13] M. J. Frisch, G. W. Trucks, H. B. Schlegel, G. E. Scuseria, M. A. Robb, J. R. Cheeseman, V. G. Zakrzewski, J. A. Montgomery, Jr., R. E. Stratmann, J. C. Burant, S. Dapprich, J. M. Millam, A. D. Daniels, K. N. Kudin, M. C. Strain, O. Farkas, J. Tomasi, V. Barone, M. Cossi, R. Cammi, B. Mennucci, C. Pomelli, C. Adamo, S. Clifford, J. Ochterski, G. A. Petersson, P. Y. Ayala, Q. Cui, K. Morokuma, D. K. Malick, A. D. Rabuck, K. Raghavachari, J. B. Foresman, J. Cioslowski, J. V. Ortiz, A. G. Baboul, B. B. Stefanov, G. Liu, A. Liashenko, P. Piskorz, I. Komaromi, R. Gomperts, R. L. Martin, D. J. Fox, T. Keith, M. A. Al-Laham, C. Y. Peng, A. Nanayakkara, M. Challacombe, P. M. W. Gill, B. Johnson, W. Chen, M. W. Wong, J. L. Andres, C. Gonzalez, M. Head-Gordon, E. S. Replogle, J. A. Pople, *GAUSSIAN 98*, Gaussian, Inc., Pittsburgh PA, **1998**.

[14] R. F. W. Bader, *Chem. Rev.* **1991**, *91*, 893−928.

[15] R. F. W. Bader, *Atoms in molecules, a Quantum Theory*, Clarendon Press, Oxford, **1990**.

[16] D. C. Fang, T. H. Tang, *AIM98PC*, Beijing Normal University, Beijing 100875, China.

[17] Available from Professor R. F. W. Bader's Laboratory, McMaster University, Hamilton, Ontario, L8S 4M1, Canada.

[18] G. Böttger, A. Geisler, E. Fröhlich, E.-U. Würthwein, *J. Org. Chem.* **1997**, *62*, 6407−6411.

Received November 24, 2002

